Geophysical Research Letters

RESEARCH LETTER
10.1029/2022GL101853

The Role of Tropical Atlantic in ENSO Predictability Barrier

Yingying Zhao[1], Yishuai Jin[2], Antonietta Capotondi[3,4], Jianping Li[5,6], and Daoxun Sun[1]

[1]Deep-Sea Multidisciplinary Research Center, Pilot National Laboratory for Marine Science and Technology (Qingdao), Qingdao, China, [2]Frontier Science Center for Deep Ocean Multispheres and Earth System (FDOMES) and PhysicalOceanography Laboratory, Ocean University of China, Qingdao, China, [3]Cooperative Institute for Research in Environmental Sciences, University of Colorado, Boulder, CO, USA, [4]Physical Sciences Laboratory, NOAA, Boulder, CO, USA, [5]Frontier Science Center for Deep Ocean Multispheres and Earth System (FDOMES) and Physical Oceanography Laboratory and Academy of the Future Ocean, Ocean University of China, Qingdao, China, [6]Laoshan Laboratory, Qingdao, China

Abstract This paper investigates the impacts of tropical Atlantic on El Niño-Southern Oscillation (ENSO) predictability through an empirical dynamical model- Linear Inverse Model (LIM). By selectively including or excluding the coupling between tropical Atlantic and tropical Pacific in LIM, we find that the tropical Atlantic dynamics significantly improve the Eastern Pacific (EP)-ENSO prediction and weaken the EP-ENSO predictability barrier (PB), with the Equatorial Atlantic (EA) mode playing a more important role than the Tropical North Atlantic (TNA) mode. The tropical Atlantic impacts on Central Pacific (CP)-ENSO predictability and PB are relatively smaller. Consistent with observations, the tropical Atlantic can weaken PB in most CMIP6 models. The evolution of the tropical Atlantic optimum initial structures confirms the important influence of the EA mode on the eastern tropical Pacific. Therefore, the tropical Atlantic dynamics, especially the EA mode, should be appropriately considered to improve the prediction of EP-ENSO and weaken the EP-ENSO PB.

Plain Language Summary El Niño–Southern Oscillation (ENSO) is one of the dominant climate modes in the tropical Pacific on interannual timescales, with significant global impacts. The tropical Atlantic sea surface temperature (SST) variability, especially in the tropical North Atlantic (TNA) and equatorial Atlantic (EA), is shown to have important impacts on ENSO variability. Using a linear dynamical model, we find that including the dynamics of the tropical Atlantic, especially the EA SST mode, can significantly improve the forecast skill of Eastern Pacific ENSO and weaken the EP-ENSO spring predictability barrier (SPB), which is a sudden reduction of ENSO prediction skill in the boreal spring. However, Central Pacific (CP)-ENSO's forecast skill is less influenced by the tropical Atlantic dynamic. Consistent with the observations, the topical Atlantic can weaken ENSO SPB in most CMIP6 climate models. Our results suggest that the tropical Atlantic dynamics should be appropriately considered to improve the forecast skill of EP-ENSO.

Key Points:

- A linear dynamical model is used to study the impact of the tropical Atlantic on El Niño-Southern Oscillation (ENSO) predictability
- Tropical Atlantic dynamics can improve Eastern Pacific (EP)-ENSO predictability and weaken EP-ENSO spring predictability barrier while the impact on Central Pacific-ENSO is limited
- The Equatorial Atlantic mode plays an important role in the tropical Atlantic influence of EP-ENSO prediction

Supporting Information:

Supporting Information may be found in the online version of this article.

Correspondence to:

Y. Jin,
jinyishuai@126.com

Citation:

Zhao, Y., Jin, Y., Capotondi, A., Li, J., & Sun, D. (2023). The role of tropical Atlantic in ENSO predictability barrier. *Geophysical Research Letters*, *50*, e2022GL101853. https://doi.org/10.1029/2022GL101853

Received 24 OCT 2022
Accepted 21 MAR 2023

1. Introduction

El Niño–Southern Oscillation (ENSO) is the dominant air-sea coupled mode in the tropical Pacific on seasonal-to-interannual timescales. ENSO drives atmospheric teleconnections that significantly impact the climate, weather, and ecosystems throughout the world (e.g., Alexander et al., 2002; Cai et al., 2019; Capotondi et al., 2020; Deser et al., 2012; Di Lorenzo et al., 2010; Liu & Di Lorenzo, 2018). According to the different longitudinal locations, ENSO events are usually classified in terms of Eastern-Pacific (EP) and Central-Pacific (CP) types (i.e., ENSO diversity; Capotondi et al., 2015, 2021). A huge effort to improve ENSO predictability and prediction has been made during the last decades (e.g., Barnston et al., 1999, 2011; Latif et al., 1998; Tang et al., 2018). According to the classic ENSO theory, key ENSO precursors are found within the Tropical Pacific basin, including the Warm Water Volume along the equatorial Pacific (Jin, 1997a, 1997b; Meinen & McPhaden, 2000), and westerly wind events in the western–central Pacific (Capotondi et al., 2018; McPhaden, 2004; Vecchi & Harrison, 2000). In addition, extratropical ENSO precursors have also been identified to play important roles in ENSO development (Capotondi & Ricciardulli, 2021; Tseng et al., 2022; Zhao et al., 2022). However, accurate ENSO forecasts several seasons in advance are still challenging (e.g., Tang et al., 2018). One significant obstacle in ENSO prediction is the so-called "spring predictability barrier" (SPB), which consists of a dramatic drop in forecast skill when the numerical ENSO predictions are made through spring (e.g., Hou et al., 2019; Jin et al., 2008, 2019, 2020; Webster & Yang, 1992; Wu et al., 2009; Xue et al., 1994).

The SPB is also known as the strong error growth in the boreal spring (Duan & Hu, 2016; Duan & Mu, 2018; Mu et al., 2007; Tao et al., 2019). Besides, previous studies have shown that the prediction of the CP type of ENSO also suffers from the summer predictability barrier (Hou et al., 2019; Ren et al., 2016).

Recent studies have highlighted the importance of the tropical Atlantic sea surface temperature (SST) variability, especially the tropical North Atlantic (TNA) and the equatorial Atlantic (EA) SST anomalies, on ENSO variability (Ding et al., 2012; Ham et al., 2013a, 2013b; Jiang & Li, 2021; Keenlyside & Latif, 2007; Keenlyside et al., 2013; Martín-Rey et al., 2012, 2014; Polo et al., 2008, 2015; Rodríguez-Fonseca et al., 2009; Wang et al., 2017). SST anomalies in the tropical North Atlantic region (TNA mode) during boreal spring could influence ENSO evolution through a subtropical teleconnection along the Pacific Intertropical Convergence Zone (ITCZ) (Ham et al., 2013a, 2013b; Wang et al., 2017). In particular, TNA SST anomalies appear to favor the development of a central Pacific (CP) type of ENSO (Ham et al., 2013b; Jiang & Li, 2021). On the other hand, variability in the eastern EA (also known as Atlantic Niño) (Zebiak, 1993), which is characterized by alternating warming/cooling phases peaking in boreal summer (Keenlyside & Latif, 2007; Xie & Carton, 2013), can affect ENSO development (Ding et al., 2012; Losada et al., 2010; Rodríguez-Fonseca et al., 2009) through shifts of the Walker circulation and associated wind anomalies over the equatorial Pacific (Ding et al., 2012; Losada et al., 2010; Polo et al., 2015; Rodríguez-Fonseca et al., 2009). EA SST anomalies are found to influence the development of the eastern Pacific (EP) type of ENSO (Ham et al., 2013b; Jiang & Li, 2021).

Since tropical Atlantic SST anomalies play an important role in ENSO variability, they may also affect ENSO predictability. The TNA and EA modes could be used as an additional predictor to improve ENSO predictability (e.g., Dommenget et al., 2006; Exarchou et al., 2021; Frauen & Dommenget, 2012; Jansen et al., 2009; Jiang & Li, 2021; Keenlyside et al., 2013; Martín-Rey et al., 2015). Using conceptual models based on parameters obtained from observations, Dommenget et al. (2006) and Jansen et al. (2009) found that the inclusion of the Atlantic Niños seems to improve the ENSO forecast skill. Frauen and Dommenget (2012) suggested that initial conditions of the tropical Atlantic may play an important role in ENSO predictability. Keenlyside et al. (2013) carried out a suite of prediction experiments with a climate model and found that the EA SST anomalies affect the development of strong El Niño events, like the 1982/83 and 1997/98 events, and significantly improve the ENSO forecast skill of these events across boreal spring, and hence may be important for weakening the SPB. Jiang and Li (2021) argued that in the real-time ENSO prediction, one should consider the pattern of the tropical Atlantic SST anomalies rather than just the TNA or EA index. Exarchou et al. (2021) used an ensemble of seasonal forecast systems and demonstrated that ENSO predictability in winter is positively correlated to the representation of equatorial Atlantic variability in summer and its teleconnection with the Pacific. However, to our knowledge, fewer studies examined the relative role of the TNA and EA in real-world ENSO prediction and SPB.

In this paper, we aim to examine the impacts of tropical Atlantic SST anomalies, especially the TNA and EA modes, on real-world CP-ENSO and EP-ENSO prediction. Here we use an empirical dynamical model, a Linear Inverse Model (LIM), to quantify the contributions of the tropical Atlantic to ENSO. LIM can successfully reproduce seasonal tropical SST variability and predictability (e.g., Penland & Matrosova, 1994; Penland & Sardeshmukh, 1995 (hereafter PS95); Newman & Sardeshmukh, 2017; Newman et al., 2011). Also, since LIMs are derived from observations, they can realistically capture interactions between different components of the climate system. Based on LIM, Zhao et al. (2022) explored the impact of the extratropical Pacific on ENSO predictability by decoupling the tropical Pacific and extratropical Pacific. In this study, we follow Zhao et al. (2022) to investigate the roles that tropical Atlantic SST modes (TNA mode and EA mode) play in ENSO predictability and SPB.

2. Data and Method

2.1. Data and Indices

Monthly mean values of SST (unit: ˚C) and SSH (unit: m) from the European Centre for Medium-Range Weather Forecasting (ECMWF) Ocean Reanalysis System 4 (ORAS4) (Balmaseda et al., 2013) for the period January 1958–December 2015 are used in this study. To test the robustness of the results, we also use monthly SST data from the National Oceanic and Atmospheric Administration (NOAA) Extended Reconstruction SST data set (ERSST) version 3 (Smith & Reynolds, 2004). Meanwhile, the monthly mean SST and SSH outputs from historical simulations (r1i1p1) of 21 climate models from phase 6 of the Coupled Model Intercomparison Project

(CMIP6) (Eyring et al., 2016) are also used (Table S1 in Supporting Information S1). The period of model data is from January 1958 to December 2014. SST and SSH fields were first averaged into 2° latitude × 5° longitude grid boxes and then the climatological seasonal cycle is removed to obtain the anomalies. The externally forced trend was removed using a method described in Text 1 in Supporting Information S1.

We use the Niño3 and Niño4 indices to represent the EP-ENSO and CP-ENSO (Hou et al., 2019; Kug et al., 2009), respectively. The Niño3 and Niño4 indices are defined as the averaged SST anomalies over the Niño3 (5°S–5°N, 150°W–90°W) and Niño4 (5°S–5°N, 160°E–150°W) regions, respectively. To assess the robustness of our results, the nearly orthogonal EP Niño index (N_{EP}) and CP Niño index (N_{CP}) defined by Ren and Jin (2011) are additionally used in this study to represent ENSO diversity: $N_{EP} = \text{Niño3} - \alpha \cdot \text{Niño4}$, $N_{CP} = \text{Niño4} - \alpha \cdot \text{Niño3}$, where $\alpha = 0.4$ when Niño4 multiplied by Niño3 is positive, otherwise $\alpha = 0$.

To evaluate the strength of the Spring/Summer predictability barrier (PB), we define the PB intensity following Jin and Liu (2021). ENSO's seasonal correlation forecast skill is a function of initial month m and lag months τ (Jin and Liu (2021); Ren et al., 2016). For every initial month m, we identify the maximum gradient of the forecast skill among the target months from February to September. Then the sum of the maximum gradient of each initial month is defined as the PB intensity.

The EA (TNA) index used in this work is defined as the averaged SST anomalies over the region 4°S–4°N, 20°W–0° (5°N–25°N, 70°W–10°W). The EA pattern and TNA pattern are obtained by regressing the corresponding indices onto tropical Atlantic SST anomalies (Figures 1a and 1b). Similarly, the leading Empirical Orthogonal Function (EOF) patterns of tropical Atlantic are obtained by regressing the corresponding Principal Component (PC) time series onto tropical Atlantic SST anomalies (Figures 1c–1f).

2.2. Constructing the LIM and Couple/Decouple Tropical Pacific and Tropical Atlantic

In systems where the nonlinear dynamics decorrelate much faster than the linear dynamics, the evolution of the climate state can be approximated as a multivariate linear dynamical system driven by white noise (Hasselmann, 1976; PS95):

$$\frac{dx}{dt} = \mathbf{L}x + \xi, \tag{1}$$

where $\mathbf{L}$ represents the linear deterministic dynamics, which can also include linearly parameterizable nonlinear dynamics, and ξ is white noise forcing. The covariance of the state vector x determines $\mathbf{L}$ (PS95):

$$\mathbf{L} = \tau_0^{-1} \ln\left\{\mathbf{C}(\tau_0)\mathbf{C}(0)^{-1}\right\}, \tag{2}$$

where $\mathbf{C}(\tau_0) = \left\langle x(t+\tau_0)x^T(t)\right\rangle$ is the lag-covariance matrix of x at lag τ_0; $\mathbf{C}(0) = \left\langle x(t)x^T(t)\right\rangle$ is the covariance matrix of x; $\tau_0 = 1$ month.

For the LIM presented in this work, we chose the state vector x:

$$x = \begin{bmatrix} \text{SST}_{\text{TP}} \\ \text{SSH}_{\text{TP}} \\ \text{SST}_{\text{TA}} \end{bmatrix}, \tag{3}$$

where SST_{TP} (SSH_{TP}) is anomalous SST (SSH) in the tropical Pacific (30°S–30°N, 130°E–70°W), SST_{TA} is anomalous SST in the tropical Atlantic (30°S–30°N, 70°W–0). Here we incorporate the tropical Pacific SSH in the LIM because the inclusion of tropical thermocline depth/SSH variability appears to significantly improve ENSO forecast skill at 6–18 months lead times (Newman et al., 2011), and is critical for capturing ENSO diversity (Capotondi & Sardeshmukh, 2015). To reduce the number of spatial degrees of freedom, x is constructed based on the PC time series of each field. We used the 10/4/6 leading PCs of $\text{SST}_{\text{TP}}/\text{SSH}_{\text{TP}}/\text{SST}_{\text{TA}}$, explaining about 77/60/71 percent of the variability of their respective fields. We reconstructed the Niño3/Niño4 indices with the leading 10 PCs of SST_{TP}, and found that they are almost the same as the original indices (Figure S1 in Supporting Information S1) with a correlation coefficient as high as 0.99. We also verified the validity of our LIM by performing a tau test (PS95), where the lag-covariances reconstructed with the LIM are compared to those computed directly from the data, as shown in Text 2 and Figure S2 in Supporting Information S1.

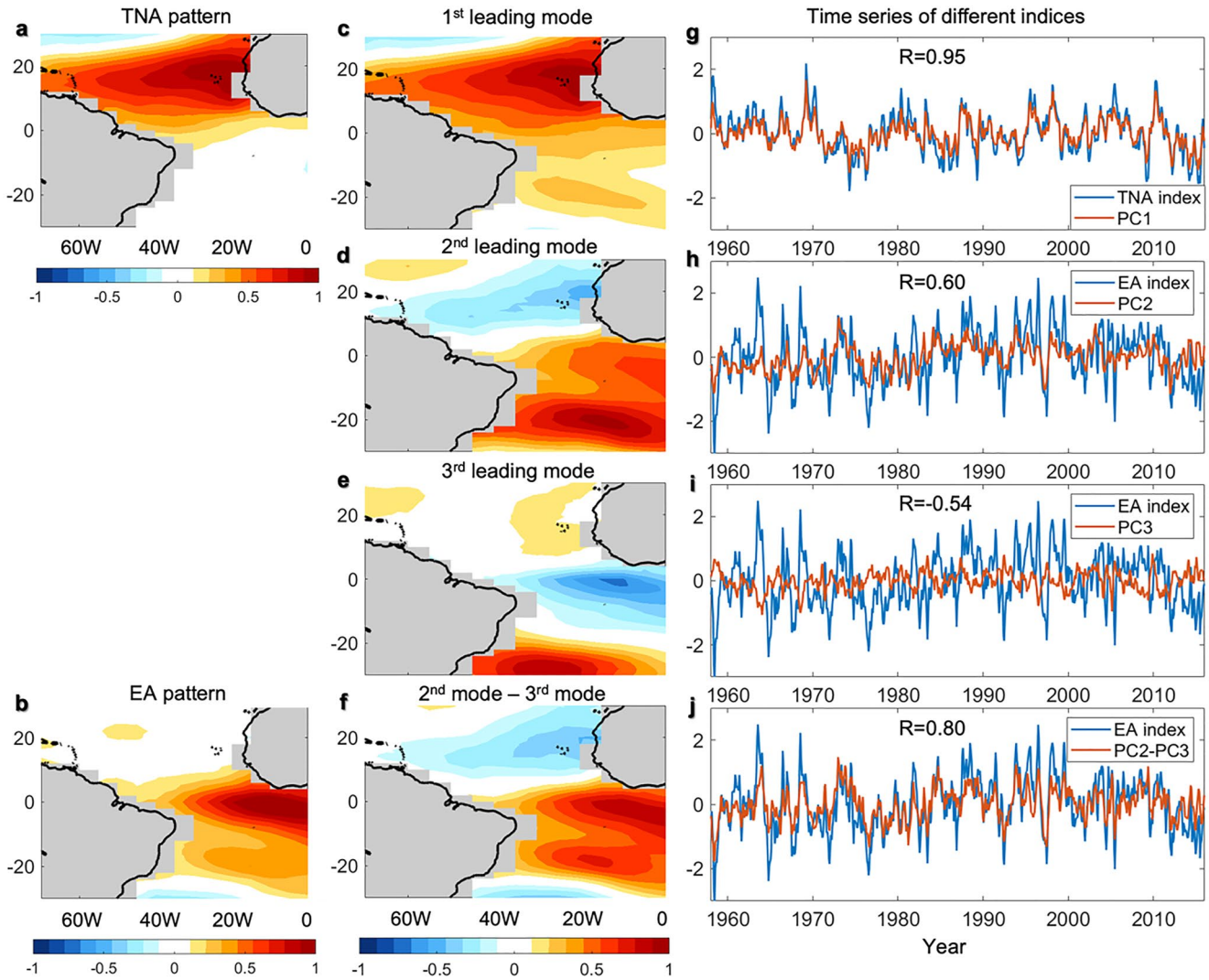

Figure 1. Regression map between the tropical Atlantic sea surface temperature (SST) anomalies and (a) Tropical North Atlantic (TNA) index, (b) Equatorial Atlantic (EA) index; (c) Spatial pattern associated with the leading Principal Component (PC) of tropical Atlantic SST anomalies; (d) Pattern associated with the second PC; (e) Spatial pattern of third PC, and (f) the difference between the spatial patterns of the second and third PCs. Time series of (g) TNA index and first PC, (h) EA index and second PC, (i) EA index and third PC, and (j) EA index and the difference between second PC and third PCs.

The dynamics of the coupled system of tropical Pacific and tropical Atlantic can be investigated by rewriting Equation 1 as:

$$\frac{dx}{dt} = \frac{d}{dt}\begin{bmatrix} x_P \\ x_A \end{bmatrix} = \begin{bmatrix} \mathbf{L_{PP}} & \mathbf{L_{AP}} \\ \mathbf{L_{PA}} & \mathbf{L_{AA}} \end{bmatrix}\begin{bmatrix} x_P \\ x_A \end{bmatrix} + \begin{bmatrix} \xi_P \\ \xi_A \end{bmatrix}, \tag{4}$$

where x_P and x_A represent the variables within the Tropical Pacific (P) and Tropical Atlantic (A), respectively. This coupled LIM is named Full LIM hereafter. In Equation 4, the sub-matrices of $\mathbf{L}$ encapsulates internal tropical Pacific processes ($\mathbf{L_{PP}}$), internal tropical Atlantic processes ($\mathbf{L_{AA}}$) and coupled dynamics ($\mathbf{L_{PA}}$ and $\mathbf{L_{AP}}$). In the full LIM, the climate dynamics of the tropical Pacific are determined by the local dynamics ($\mathbf{L_{PP}}x_P$) and the tropical Atlantic teleconnection ($\mathbf{L_{AP}}x_A$):

$$\frac{dx_P}{dt} = \mathbf{L_{PP}}x_P + \mathbf{L_{AP}}x_A + \xi_P. \tag{5}$$

To remove the coupling effects between tropical Pacific and tropical Atlantic, we construct a No-Tropical Atlantic LIM (No-TA LIM) by setting the coupling dynamics $\mathbf{L_{AP}} = \mathbf{L_{PA}} = \mathbf{0}$ in $\mathbf{L}$. Then the tropical Pacific system is described as:

$$\frac{dx_P}{dt} = \mathbf{L_{PP}} x_P + \xi_P. \tag{6}$$

Note that retaining different EOF numbers in the state vector x doesn't significantly change the tropical Pacific SST variance pattern in the Full-LIM/No-TA LIM (see Text S3 and Figure S3 in Supporting Information S1), confirming the robustness of the LIMs.

To separate the influence of the EA and TNA modes on ENSO predictability in the LIM, we relate these modes to the EOF modes of tropical Atlantic SST anomalies (Figure 1). We find that the dominant EOF pattern of the tropical Atlantic (Figure 1c) is similar to the TNA pattern (Figure 1a), and the corresponding PC time series is highly correlated with the TNA index ($R = 0.95$, Figure 1g). The second (third) leading PC time series shows a positive (negative) correlation with the EA index (Figures 1h and 1i), and the difference between PC2 and PC3 yields a time series that is highly correlated with the EA index ($R = 0.80$, Figure 1j). The corresponding regression pattern of PC2 minus PC3 (Figure 1f) also shares common features with the EA pattern (Figure 1b). Therefore, in this study, we use the dominant PC time series of tropical Atlantic to represent the TNA mode and use the time series of PC2-PC3 to represent the EA mode.

Like the No-TA LIM, we build No-PC1 LIM (No-PC2&3 LIM) where we remove the impact of the TNA mode (EA mode) on the tropical Pacific climate variability by zeroing out the submatrix representing coupling dynamics between PC1 (PC2 and PC3) of tropical Atlantic and tropical Pacific in the dynamical operator $\mathbf{L}$ of the Full LIM.

The approaches used to make predictions and to identify the "optimal" initial condition for anomaly growth using the LIM are very similar to those described in Zhao et al. (2022). More details can be found in Text S4 in Supporting Information S1.

3. The Role of Tropical Atlantic in CP and EP ENSO Prediction and PB

3.1. The Overall Role of the Tropical Atlantic

We start by evaluating the general impact of the tropical Atlantic on predicting EP-ENSO and CP-ENSO. Figure S4 in Supporting Information S1 shows the comparison of Niño3/Niño4 ENSO forecast skills predicted by different LIMs. The Full LIM, which includes the impacts of the tropical Atlantic, exhibits the best prediction skill compared to the decoupled LIMs (blue line in Figure S4 in Supporting Information S1). While the No-TA LIM, in which all the interactions between tropical Atlantic and tropical Pacific are missing, shows the worst forecast skill (red line in Figure S4 in Supporting Information S1).

The tropical Atlantic generally shows a minor (major) influence on Niño4 (Niño3) prediction skills. Specifically, the tropical Atlantic impacts the forecast skill of CP-ENSO only at longer lead times (>6 months), and the difference in ACC skills between No-TA LIM and Full LIM is very small (<0.1) (blue line and red line in Figure S4a in Supporting Information S1). For the EP-ENSO, the ACC skill in No-TA LIM (red line in Figure S4b in Supporting Information S1) decreases significantly faster than that of Full LIM (blue line in Figure S4b in Supporting Information S1) after 3 months' prediction, and the difference between them is about 0.2 on longer time scales (>6 months). Note that the results are not qualitatively changed when we use N_{EP} and N_{CP} indices to represent ENSO diversity (Figures S4c and S4d in Supporting Information S1).

To explore the impacts of the tropical Atlantic on the Spring/Summer PB, we compare seasonal correlation forecast skills of the ENSO indices predicted by different LIMs (Figure 2). Note that Steiger's Z-test (Steiger, 1980) is used to test the significance level of the differences between seasonal forecast skills predicted by different LIMs (Figures 2d, 2h, and Figures 2j, 2l, 2n, 2p). Black dots in these figures show the differences significant at 90% level. The predictability maps represent the forecast skills as a function of the lead time (x-axis) and the initial calendar month (y-axis).

For the CP-ENSO (Niño4 index), by decoupling the tropical Pacific and tropical Atlantic (No-TA LIM), the forecast skill is reduced compared to the Full LIM (Figure 2a vs. Figure 2c), especially when the initial month

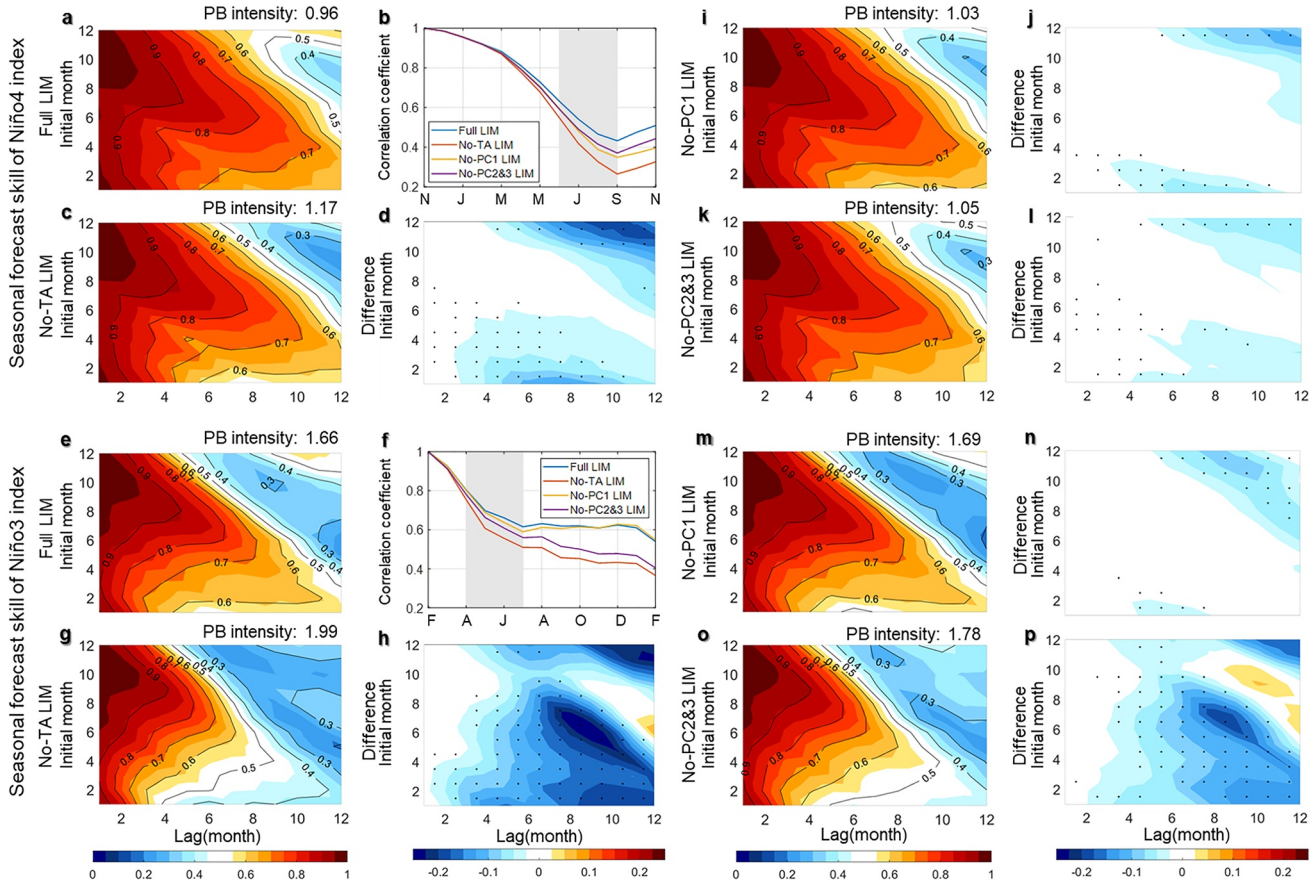

Figure 2. The seasonal correlation forecast skill of the Niño4 as a function of the initial calendar month (*y*-axis) and lag month (*x*-axis) predicted by (a) Full Linear Inverse Model (LIM), (c) No-TA LIM, (i) No-PC1 LIM, and (k) No-PC2&3 LIM. (b) Correlation forecast skills of the Niño4 index predicted from February in Full LIM (blue line), No-TA LIM (red line), No-PC1 LIM (orange line), and No-PC2&3 LIM (purple line). Difference of seasonal Niño4 index forecast skill between (d) No-TA LIM and Full LIM, (j) No-PC1 LIM and Full LIM, (l) No-PC2&3 LIM and Full LIM. Black dots show the differences past the 90% significant level of Steiger's Z-test. (e–h) and (m–p) Same as (a–d) and (i–l) but for Niño3 index seasonal forecast skill.

is in boreal winter (November to February) at 8–12 months lead (Figure 2d), leading to a stronger PB in No-TA LIM (PB intensity: 1.17) compared to the Full LIM (PB intensity: 0.96) (Figure 2c). To further identify the role of tropical Atlantic in CP-ENSO PB, we compare the Niño4 index forecast skill predicted from November in different LIMs (Figure 2b). The ACC skill in No-TA LIM (red line in Figure 2b) shows a stronger Summer PB compared to the Full LIM (blue line in Figure 2b) from June to August (the gray shading in Figure 2b). Similar results can be obtained from the forecast skills predicting from December (Figure S5c in Supporting Information S1). Therefore, the tropical Atlantic can weaken the Summer PB of the CP-ENSO.

For EP-ENSO (Niño3 index), when removing the interactions between tropical Pacific and tropical Atlantic (No-TA LIM, Figure 2g), the seasonal forecast skill is largely decreased compared to the Full system (Figure 2e). The PB intensity is much larger in the No-TA LIM (1.99) compared to the Full LIM (1.66). In No-TA LIM, the ACC is about 0.4 at 6 months lead-time when the initial month is January (Figure 2g), which is smaller compared to the Full LIM (about 0.6 in Figure 2e). Specifically, the ACC skills of the Niño3 index when the initial month is February show that the dynamics between tropical Pacific and tropical Atlantic can largely weaken the EP-ENSO SPB (Figure 2f). When decoupling tropical Atlantic and tropical Pacific, the ACC skill in No-TA LIM (red line in Figure 2f) shows a stronger SPB, decreasing faster compared to the Full LIM (blue line in Figure 2f) during boreal spring and summer. Seasonal prediction skills show similar results when the initial month is January (Figure S5d in Supporting Information S1). The largest impact of tropical Atlantic on EP-ENSO seasonal predictability is located when the initial month is from June to July at 7–10 months lead (Figure 2h), in the following spring season. This can be seen clearly in Figure S5e in Supporting Information S1 which shows the Niño3 index seasonal forecast skill when the initial month is July. The forecast skill drops dramatically during

the following spring season (gray shading in Figure S5e in Supporting Information S1), which is also an SPB problem. Therefore, the tropical Atlantic plays an important role in weakening the EP-ENSO SPB.

Our result shows that the predictability of CP-ENSO is higher than EP-ENSO, which is consistent with previous studies using dynamical models (e.g., Figures 3a and 3b in Kim et al., 2009), statistical models (e.g., Tseng et al., 2022; Zhao et al., 2022), and the information theory-based framework (Fang & Chen, 2022). Meanwhile, a well-known phenomenon is that EP El Niño events are more predictable than CP El Niño events (e.g., Zheng & Yu, 2017). It should be noted here that the predictability of EP/CP ENSO indices identified in this paper is not the same as the predictability of EP/CP El Niño events. On the other hand, based on dynamical models, some previous studies also indicated that the EP-ENSO has a relatively higher prediction skill than the CP-ENSO (e.g., Jeong et al., 2012, 2015; Ren et al., 2017). However, dynamical prediction systems are often deficient in their simulation of ENSO diversity (Capotondi et al., 2020), a factor that may contribute to their difficulty in predicting that diversity.

To further identify the role of tropical Atlantic in ENSO prediction, we build LIMs from the output of each CMIP6 model (Table S1 in Supporting Information S1) and repeated the observational LIM analysis. The arithmetic mean of the forecast skills in each model determines the multi-model ensemble mean (MEM) statistics. In the Full LIM, most CMIP6 models show a weaker PB intensity (Figure S6 in Supporting Information S1, purple bars) compared to the observation (green line in Figure S6 in Supporting Information S1), and so does the MEM. Removing the impacts of the tropical Atlantic increases the PB intensity in most CMIP6 models. For the MEM, the PB intensities of both Niño4 and Niño3 indices in the No-TA LIM are increased compared to those in the Full LIM. This is consistent with the observations but the increases in MEM are smaller. These increases in MEM are supported by a strong inter-model consensus, with 19 out of 21 models (90%) for the Niño4 index and 18 out of 21 models (86%) for the Niño3 index (Figure S6 in Supporting Information S1). This suggests that the tropical Atlantic can weaken the ENSO PB in most models. To sum up, although most models underestimate the PB intensity, the tropical Atlantic contributes to weakening the ENSO PB in most CMIP6 models as in the ORAS4 reanalysis.

3.2. The Respective Role of TNA and EA Modes in ENSO Prediction and PB

To distinguish which Atlantic SST mode (EA mode/TNA mode) is more important for ENSO prediction and PB, we further examine the forecast skills of the ENSO indices in the No-PC1 LIM/No-PC2&3 LIM where the interactions between TNA/EA mode and tropical Pacific are removed.

For CP-ENSO (Niño4 index), the prediction skill in No-PC1 LIM and No-PC2&3 LIM is comparable, indicating that the EA mode and TNA mode make a comparable contribution to CP-ENSO predictability (purple line and orange line in Figure S4a in Supporting Information S1). For EP-ENSO (Niño3 index), when we only decouple the TNA mode, the No-PC1 LIM (orange line in Figure S4b in Supporting Information S1) shows similar forecast skill to the Full LIM (blue line in Figure S4b in Supporting Information S1), which means that the TNA mode has little influence on Niño3 index forecast skill. However, when the dynamics of the EA mode are removed, the Niño3 index prediction in the No-PC2&3 LIM is significantly decreased compared to the Full LIM (purple line vs. blue line in Figure S4b in Supporting Information S1), suggesting that the EA mode plays an important role in enhancing the EP-ENSO predictability. Note that the results are not qualitatively changed when we use the N_{EP} and N_{CP} indices to represent ENSO diversity (Figures S4c and S4d in Supporting Information S1).

For the seasonal forecast skill of CP-ENSO (Niño4 index), the No-PC1 LIM and No-PC2&3 LIM exhibit similar ACC skills (Figure 2i vs. Figure 2k), which suggests that the TNA and EA modes may play comparable roles in the seasonal predictability of CP-ENSO. This can also be seen in the seasonal prediction skills starting from November or December (Figure 2b and Figure S5d in Supporting Information S1). The differences between No-PC1 LIM/No-PC2&3 LIM and Full LIM are subtle (Figures 2j and 2l), indicating that the impact of the tropical Atlantic SST modes on CP-ENSO seasonal predictability is small.

For the seasonal forecast skill of EP-ENSO (Niño3 index), when only decoupling the TNA SST mode, the No-PC1 LIM (Figure 2m) shows ACC skills similar to the Full LIM (see their differences in Figure 2n), suggesting that the TNA mode plays a minor role in EP-ENSO seasonal predictability. However, when we decouple the EA mode of tropical Atlantic, the ACC skill of Niño3 index is significantly decreased compared to the Full LIM (Figure 2p), especially during boreal spring and summer, leading to a stronger SPB in the No-PC2&3 LIM (Figure 2o).

Specifically, the Niño3 index forecast skill predicted from February in No-PC2&3 LIM when decoupling the EA mode shows stronger SPB compared to the Full LIM (purple and blue lines in Figure 2f), while the No-PC1 LIM (orange line in Figure 2f) exhibits a similar forecast skill to the Full LIM (blue line in Figure 2f) when only decoupling the TNA mode. Similar results are also obtained when predicting from January (Figure S5d in Supporting Information S1). Given the above, tropical Atlantic SST is important for weakening the EP-ENSO SPB, with the EA SST mode playing the dominant role.

Note that the impact of the EA mode on EP-ENSO seasonal predictability is more effective at 7–10 months lead when predicting from boreal summer (June to August, Figure 2p), which is consistent with the fact that the EA mode peaks in boreal summer (Keenlyside & Latif, 2007; Xie & Carton, 2013). The major improvement of the EP-ENSO prediction from boreal summer occurs in the following spring season (Figure S5e in Supporting Information S1), after ENSO's mature phase. This is consistent with previous studies showing that the Atlantic Ocean plays an important role in the decay phase of El Niño. Specifically, the SST anomalies in the Atlantic Ocean can drive easterly anomalies over the equatorial western Pacific during the decay phase of El Niño, which induce an upwelling oceanic Kelvin wave, accelerating its demise (e.g., Kim & Yu, 2022).

In all, the tropical Atlantic exhibits a minor (major) impact on CP-ENSO (EP-ENSO) predictability and PB. Specifically, for CP-ENSO, the EA and TNA modes tend to play comparable roles in enhancing predictability and weakening PB. On the other hand, the EA mode is much more important than the TNA mode in improving EP-ENSO prediction skills and crossing the SPB. To test the robustness of our results, we repeat the LIM calculations using the NOAA ERSST v3 instead of the ORAS4 SST, and find that different observational products do not qualitatively change our results (Figures S7 and S8 in Supporting Information S1). Note that we also examine the seasonal forecast skill of the N_{CP} and N_{EP} indices in different LIMs (Figures S9–S11 in Supporting Information S1), and obtain similar impacts of the tropical Atlantic on the seasonal predictability of ENSO diversity.

4. The Optimum Initial Condition of Central and Eastern Tropical Pacific

To further clarify the physical processes through which the tropical Atlantic influences the CP-ENSO-like mode and EP-ENSO-like mode, we compare the optimum initial conditions for the growth of SST anomalies in the Niño3 and Niño4 regions in different LIMs and explore how they evolve with time. Note that the optimal initial structures have arbitrary units (Figure 3 and Figure S12 in Supporting Information S1), but the normalization is consistent among panels so that the amplitudes are comparable.

4.1. The Optimum Initial Condition of Central Equatorial Pacific

First, we examine the tropical Atlantic initial condition of the Niño4 region and how it evolves. The "Maximum amplification" (MA) (PS95) curve for SST anomaly growth in the Niño4 region (Figure S13a in Supporting Information S1) shows that the maximum growth in Full LIM is achieved at a lag of about 8 months. Therefore, $\tau = 8$ months is chosen to calculate the optimal initial condition in the tropical Atlantic. The tropical Atlantic optimal initial condition in the Full LIM (Figure 3a) resembles the typical TNA mode in the Tropical North Atlantic region (Ham et al., 2013a, 2013b). There is also a warm center in the equatorial region, which is similar to the EA mode, and a stronger warm center in the Tropical South Atlantic region (Figure 3a). Then we integrate the basic equation of LIM (Equation 1) using the tropical Atlantic initial condition (with no signal in the tropical Pacific) to see the progression. After 3 months of evolution, a weak cooling signal appears in the eastern tropical Pacific region but not in the central tropical Pacific (Figure 3b). The cooling signal is then amplified by the local dynamics in the tropical Pacific (Figure 3c) and finally evolves into a mature ENSO mode after about 9 months (Figure 3d). This suggests that even without an initial signal in the tropical Pacific, only perturbations in the tropical Atlantic SST could drive SST anomalies in the tropical Pacific.

To determine the individual impact of the EA mode and the TNA mode on SST anomaly growth in the Niño4 region, we compare the tropical Atlantic initial condition and its time evolution in No-PC1 LIM (Figures 3e–3h) and No-PC2&3 LIM (Figures 3i–3l). In No-PC1 LIM, the initial condition is similar to the Full LIM in equatorial Atlantic and tropical South Atlantic regions, while the TNA-like pattern in the Full LIM is much weaker (Figure 3e vs. Figure 3a). In No-PC2&3 LIM, the initial condition exhibits TNA-like pattern in the tropical North Atlantic region, which is similar to the Full LIM, while the EA-like pattern is missing in equatorial Atlantic compared to the Full LIM (Figure 3i vs. Figure 3a). After 3 months' evolution, a weak cooling signal appears

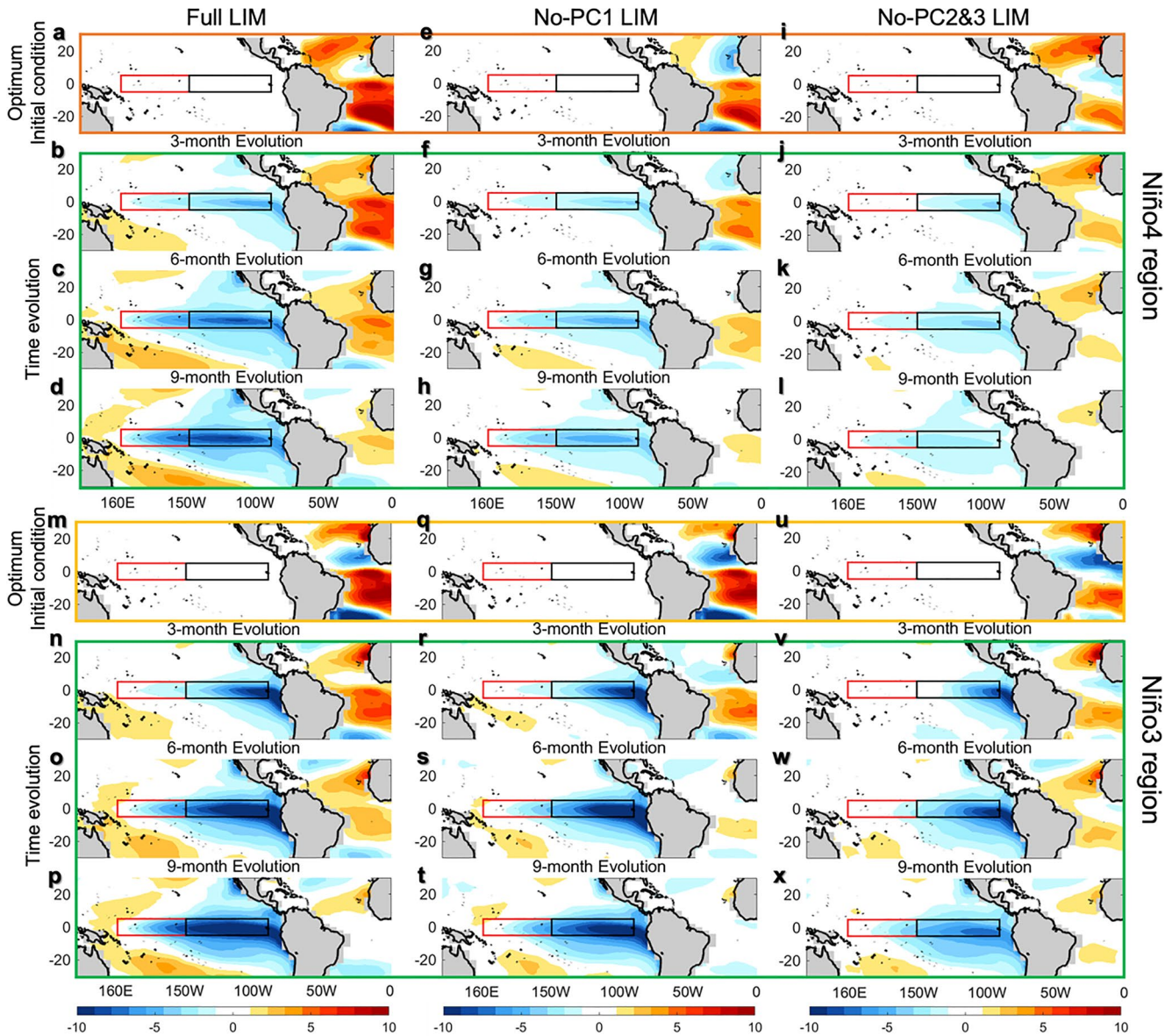

Figure 3. (a) The 8-month tropical Atlantic optimal initial structure of SST variances in the Niño4 region and (b–d) its time evolution from 3 to 9 months in the Full Linear Inverse Model (LIM). Figures (e–h) and (i–l) are similar to (a–d), except for the optimal initial structure and time evolutions in No-PC1 LIM and No-PC2&3 LIM, respectively. (m) The 6-month tropical Atlantic optimal initial structure of SST variances in the Niño3 region and (n–p) its time evolution from 3 to 9 months in the Full LIM. Figures (q–t) and (u–x) are similar to (m–p), except for the optimal initial structure and time evolutions in No-PC1 LIM and No-PC2&3 LIM, respectively.

in the eastern tropical Pacific region in both No-PC1 LIM and No-PC2&3 LIM (Figures 3f and 3j). Then the cooling signal develops into an ENSO-like pattern after 9 months (Figures 3g–3h and 3k–3l), with a smaller SST variability compared to the mature phase in Full LIM (Figure 3d), suggesting that both the EA mode and the TNA mode are important for the ENSO development.

Interestingly, during the development process of ENSO, the SST variability in the Niño3 region (black square in Figures 3a–3l) is much stronger than that in the Niño4 region (red square in Figures 3a–3l). That is, the optimum initial condition in tropical Atlantic that maximizes the growth of SST variance in the Niño4 region can drive even stronger signals in the Niño3 region, indicating the much more important role played by the tropical Atlantic in energizing EP-ENSO compared to CP-ENSO. This is consistent with Section 3 that the contribution of tropical Atlantic SST to the CP-ENSO predictability is comparatively smaller (Figure S4 in Supporting Information S1

and Figure 2). Moreover, the SST signal in the Niño4 region is very weak in the evolution at month 3 (red square in Figures 3b, 3f and 3j) and becomes stronger at month 6 (red square in Figures 3c, 3g and 3k), explaining the previous finding that the tropical Atlantic mainly influences the forecast skill of CP-ENSO at time scales longer than 6 months (Figure S4a in Supporting Information S1).

4.2. The Optimum Initial Condition of Eastern Equatorial Pacific

Generally, the tropical Atlantic optimum initial condition for the Niño3 region can drive much stronger SST anomalies in the tropical Pacific compared to that for the Niño4 region (Figures 3m–3x vs. Figures 3a–3l). For the Niño3 region, since the maximum growth rate of the MA curve (Figure S13b in Supporting Information S1) occurs at about 6 months, we use $\tau = 6$ months to calculate the tropical Atlantic optimum initial condition for SST anomaly growth. In the Full LIM, the initial condition (Figure 3m) is similar to that for the Niño4 region (Figure 3a) in the tropical South Atlantic but shows a dipole structure in the tropical North Atlantic instead of the TNA-like pattern in the initial condition for the Niño4 region (Figure 3m vs. Figure 3a). The tropical Atlantic dynamics drive strong EP-ENSO-like variance in the eastern tropical Pacific after 3 months (Figure 3n), which further develops into an EP-ENSO-like mode after 6 months (Figure 3o) and extends further westward toward the central tropical Pacific after 9 months (Figure 3p). The SST signal in the Niño3 region driven by the tropical Atlantic after 3 months' evolution is strong so that the tropical Atlantic can significantly influence the EP-ENSO predictability on shorter time scales (~3 months) (Figure S4b in Supporting Information S1) and can influence the SPB when the initial month is in boreal spring (Figures 2e–2h).

In the No-PC1 LIM where the impact of the TNA mode is removed, the initial condition is similar to the Full LIM but with a weaker warming center in the tropical North Atlantic (Figure 3q vs. Figure 3m), driving a strong cooling signal in the eastern tropical Pacific with comparable amplitude to that in the Full LIM after 3/6/9 months of evolution (Figures 3r–3t vs. Figures 3n–3p). This indicates that the TNA mode may play a less important role in the development of the EP-ENSO-like mode. In No-PC2&3 LIM, the initial condition exhibits a dipole structure in the tropical North Atlantic region, which is similar to the Full LIM, while the EA-like pattern in the equatorial Atlantic is missing compared to the Full LIM (Figure 3u vs. Figure 3m). After 3/6/9 months of evolution, the initial condition drives much weaker cooling anomalies in the eastern tropical Pacific compared to the Full LIM (Figures 3v–3x vs. Figures 3n–3p), which suggests that the EA mode is very important to the development of EP-ENSO-like mode. Therefore, the EA mode contributes more to the development and prediction of EP-ENSO-like mode compared to the TNA mode, explaining the important role that the EA mode plays in impacting the EP-ENSO SPB (Figures 2m–2p).

5. Summary and Discussion

This paper quantifies the role of the tropical Atlantic SST anomalies, especially the TNA and EA modes, in predicting CP-ENSO and EP-ENSO and weakening the PB. We use an empirical dynamical model—LIM—that allows us to selectively and objectively include or exclude the tropical coupling between the Atlantic and Pacific instead of simple linear regressions as in many previous studies. Moreover, the LIM is not a purely linear model, as it includes a stochastic forcing term that encapsulates fast system nonlinearities. It has been shown that its prediction skill in the tropical Pacific is comparable to that of state-of-the-art operational forecast systems like the National Multi-Model Ensemble (NMME) (Newman & Sardeshmukh, 2017). Concerning our LIM, its ability to correctly reproduce the instantaneous and lag-covariances of observations (Figure S2 in Supporting Information S1) provides confidence that it encapsulates the correct feedback among different variables.

In this work, we focus on the effect of the tropical Atlantic on ENSO PB, which is much less studied. We find that the tropical Atlantic dynamics play an important role in predicting the EP-ENSO at timescales longer than 3 months (Figures S4b and S4d in Supporting Information S1, and Figures 3m–3x), and can weaken the EP-ENSO SPB (Figures 2e–2h), with the EA mode playing the dominant role (Figures 2m–2p). Although the tropical Atlantic impact on CP-ENSO predictability is comparatively smaller and occurs primarily on longer timescales (>6 months) (Figure S4a in Supporting Information S1 and Figures 3a–3l), the tropical Atlantic can also weaken the CP-ENSO PB (Figures 2a–2d). These results do not qualitatively change with different observational products (Figures S7 and S8 in Supporting Information S1). Furthermore, the weakening effects of tropical Atlantic dynamics on CP-ENSO/EP-ENSO PB are supported by the result obtained with CMIP6 models, with a

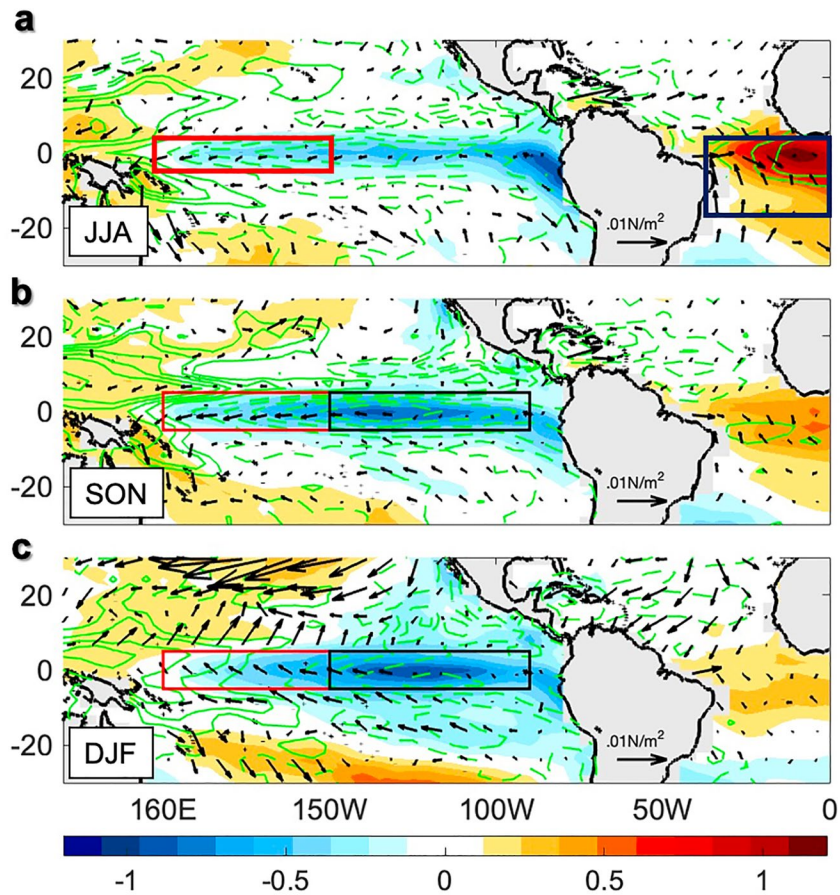

Figure 4. Linear partial regression maps between the JJA Equatorial Atlantic (EA) index and seasonal sea surface temperature (SST) anomalies/SSH anomalies and the corresponding wind stress anomalies during (a) June–August, (b) September–November, and (c) December–February. To remove the oscillatory effect of El Niño-Southern Oscillation itself, a regression on the previous year's wintertime Niño3.4 index is subtracted from the JJA EA index. The shadings/contours show the SST/SSH anomalies. For the contours, solid and dashed lines show positive and negative values, respectively. The interval is 0.1.

strong inter-model consensus, although many of the models tend to underestimate the PB intensity (Figure S6 in Supporting Information S1).

To further explore how the EA mode impacts the development of ENSO, we investigate the evolution patterns of the EA mode during its most active seasons (summer), to clarify the physical mechanisms through which it impacts ENSO in the subsequent seasons (Figure 4). In the boreal summer for an Atlantic Niño (JJA; Figure 4a), there is a significant positive SST anomaly over the equatorial Atlantic region. The anomalous warming induces wind convergence locally (black box in Figure 4a), which enhances the Walker circulation and generates westward wind anomalies in the equatorial western Pacific (red box in Figure 4a) (Ding et al., 2012; Polo et al., 2015). These easterlies contribute to extend the eastern Pacific Cold Tongue westward (Figure 4b), favoring the development of La Niña events with cold anomalies in both the Niño4 (red boxes in Figures 4b and 4c) and Niño3 (black boxes in Figures 4b and 4c) regions. The corresponding SSH anomalies are also shown in Figure 4 as contours. Note that the maximum effect of JJA EA on the following seasons is in the eastern tropical Pacific (i.e., Niño3 region). It is consistent with the results that EA plays a more important role in the EP-ENSO prediction than in the CP-ENSO (Figure 2p vs. Figure 2l). The possible reason is that the EA mode induces wind anomalies that alter the thermocline depth in the far eastern and western Pacific, and the zonal thermocline slope (Ding et al., 2012). These conditions may favor the development of EP-ENSO events in the absence of extra-tropical Pacific precursors (Capotondi & Ricciardulli, 2021; Capotondi & Sardeshmukh, 2015). The EA and TNA modes impact the ENSO variability through substantially different physical processes, which may lead to their different roles in ENSO prediction. Specifically, the EA mode modulates the ENSO variability by altering the Walker circulation

(Ding et al., 2012; Losada et al., 2010; Polo et al., 2015; Rodríguez-Fonseca et al., 2009), while the TNA mode affects the tropical Pacific variability along the Pacific ITCZ (Ham et al., 2013a).

Our results suggest that EP-ENSO can be more predictable and the PB can be weakened when the dynamics of the tropical Atlantic are appropriately considered. The full optimal initial structures including both tropical Pacific and tropical Atlantic and their time evolution are shown in Figure S12 in Supporting Information S1. The optimal anomalies and their evolution are in the tropical Pacific much stronger compared to those in the tropical Atlantic basin (Figure S12 in Supporting Information S1 vs. Figure 3). However, despite the small tropical Atlantic signal in the initial optimal structure (relative to the Pacific), the tropical Atlantic can still make a significant impact on the predictability of EP events (Figures 2e–2h). Capotondi and Ricciardulli (2021) showed significant correlations between CP events and extra-tropical Pacific ENSO precursors, which were missing for EP events. As seen in this study, the important role of the tropical Atlantic in the development of EP events may be responsible for the initiation of these events.

Note that we only explicitly examine the impact of the tropical Atlantic in this paper, but other influences (e.g., extratropical Pacific) are not explicitly considered. Extratropical Pacific dynamics like the North and South Pacific Meridional Modes have been shown to greatly impact ENSO predictability and PB (Ren et al., 2019; Zhao et al., 2022). These influences can be expected to be implicitly included in the LIM, because the tropical Pacific region we used to construct the LIM is from 30°S to 30°N, and the SST PCs over this region are correlated with the extratropical Pacific PCs. The dynamics of different regions are not completely independent of each other, but LIM gives us an approach to decouple parts of the system. How to quantitatively describe the combined/respective effects of these areas on ENSO prediction requires further studies.

Another interesting question is how tropical Atlantic dynamics impact the prediction of different phases of ENSO (i.e., El Niño and La Niña). This question deserves to be explored in depth. However, given the relatively short duration of the observational data, the number of El Niño/La Niña developing years is insufficient to obtain robust results. Long climate model simulations may be suitable candidates for future studies.

We note here that the influence of the tropical Atlantic on ENSO may include nonlinearities that LIM cannot capture. On the other hand, Coupled General Circulation Models (CGCMs) utilized to address these issues through basin decoupling or partially coupled experiments (e.g., Rodriguez-Fonseca et al., 2009; Ding et al., 2012; Keenlyside et al., 2013) may have biases that can limit the reliability of the results. Thus, close comparisons of results obtained with the LIM versus those obtained with the CGCMs may help identify the most robust aspects of the Atlantic influence on ENSO. This avenue for further exploration of inter-basin interactions will be pursued in future work.

Data Availability Statement

The ORAS4 output can be downloaded from: https://www.cen.uni-hamburg.de/en/icdc/data/ocean/easy-init-ocean/ecmwf-ocean-reanalysis-system-4-oras4.html. The ERSST v3 observation data are available online: https://www.ncei.noaa.gov/access/metadata/landing-page/bin/iso?id=gov.noaa.ncdc:C00833. The CMIP6 data were obtained from https://esgf-node.llnl.gov/projects/cmip6/. The specific CMIP6 models used in this paper can be found in Table S1 in Supporting Information S1.

Acknowledgments
We thank two anonymous reviewers and editor for their constructive comments on this paper. This work is supported by Chinese NSFC42206025, Chinese NSFC42206013, and Shandong Provincial Natural Science Foundation, China, ZR202102240275. AC was supported by the NOAA Climate Program Office Climate Variability and Predictability Program.

References

Alexander, M. A., Bladé, I., Newman, M., Lanzante, J. R., Lau, N.-C., & Scott, J. D. (2002). The atmospheric bridge: The influence of ENSO teleconnections on air–sea interaction over the global oceans. *Journal of Climate*, *15*(16), 2205–2231. https://doi.org/10.1175/15200442(2002)015,2205:TABTIO.2.0.CO;2

Balmaseda, M. A., Mogensen, K., & Weaver, A. T. (2013). Evaluation of the ECMWF ocean reanalysis system ORAS4. *Quarterly Journal of the Royal Meteorological Society*, *139*(674), 1132–1161. https://doi.org/10.1002/qj.2063

Barnston, A. G., Tippett, M. K., L'Heureux, M. L., Li, S., & DeWitt, D. G. (2011). Skill of real-time seasonal ENSO model predictions during 2002–11: Is our capability increasing? *Bulletin of the American Meteorological Society*, *93*(5), 631–651. https://doi.org/10.1175/bams-d-11-00111.2

Barnston, A. G., Glantz, M. H., & He, Y. (1999). Predictive skill of statistical and dynamical climate models in SST Forecasts during the 1997–98 El Niño episode and the 1998 La Niña onset. *Bulletin of the American Meteorological Society*, *80*(2), 217–244. https://doi.org/10.1175/1520-0477(1999)080<0217:psosad>2.0.co;2

Cai, W., Wu, L., Lengaigne, M., Li, T., McGregor, S., Kug, J. S., et al. (2019). Pantropical climate interactions. *Science*, *363*, eaav4236.

Capotondi, A., Deser, C., Phillips, A. S., Okumura, Y., & Larson, S. M. (2020). ENSO and Pacific decadal variability in the community Earth system model version 2. *Journal of Advances in Modeling Earth Systems*, *12*, e2019MS002022. https://doi.org/10.1029/2019ms002022

Capotondi, A., & Ricciardulli, L. (2021). The influence of Pacific winds on ENSO diversity. *Scientific Reports*, *11*(1), 18672. https://doi.org/10.1038/s41598-021-97963-4

Capotondi, A., & Sardeshmukh, P. D. (2015). Optimal precursors of different types of ENSO events. *Geophysical Research Letters*, *42*(22), 9952–9960. https://doi.org/10.1002/2015gl066171

Capotondi, A., Sardeshmukh, P. D., & Ricciardulli, L. (2018). The nature of the stochastic wind forcing of ENSO. *Journal of Climate*, *31*(19), 8081–8099. https://doi.org/10.1175/JCLI-D-17-0842.1

Capotondi, A., Wittenberg, A. T., Kug, J.-S., Takahashi, K., & McPhaden, M. (2021). ENSO diversity. In M. J. McPhaden, A. Santoso, & W. Cai (Eds.), *El Niño southern oscillation in a changing climate* (pp. 65–86). American Geophysical Union (AGU).

Capotondi, A., Wittenberg, A. T., Newman, M., Di Lorenzo, E., Yu, J.-Y., Braconnot, P., et al. (2015). Understanding ENSO diversity. *Bulletin of the American Meteorological Society*, *96*(6), 921–938. https://doi.org/10.1175/bams-d-13-00117.1

Deser, C., Phillips, A. S., Tomas, R. A., Okumura, Y. M., Alexander, M. A., Capotondi, A., et al. (2012). ENSO and Pacific decadal variability in the community climate system model version 4. *Journal of Climate*, *25*(8), 2622–2651. https://doi.org/10.1175/jcli-d-11-00301.1

Di Lorenzo, E., Cobb, K. M., Furtado, J. C., Schneider, N., Anderson, B. T., Bracco, A., et al. (2010). Central Pacific El Nino and decadal climate change in the North Pacific ocean. *Nature Geoscience*, *3*(11), 762–765. https://doi.org/10.1038/ngeo984

Ding, H., Keenlyside, N. S., & Latif, M. (2012). Impact of the equatorial Atlantic on the El Niño southern oscillation. *Climate Dynamics*, *38*(9–10), 1965–1972. https://doi.org/10.1007/s00382-011-1097-y

Dommenget, D., Semenov, V., & Latif, M. (2006). Impacts of the tropical Indian and Atlantic oceans on ENSO. *Geophysical Research Letters*, *33*(11), L11701. https://doi.org/10.1029/2006gl025871

Duan, W., & Mu, M. (2018). *Predictability of El Niño-southern oscillation events*. Oxford Research Encyclopedia of Climate Science.

Duan, W. S., & Hu, J. Y. (2016). The initial errors that induce a significant "spring predictability barrier" for El Niño events and their implications for target observation: Results from an eaEarthystem model. *Climate Dynamics*, *46*(11–12), 3599–3615. https://doi.org/10.1007/s00382-015-2789-5

Exarchou, E., Ortega, P., Rodríguez-Fonseca, B., Losada, T., Polo, I., & Prodhomme, C. (2021). Impact of equatorial Atlantic variability on ENSO predictive skill. *Nature Communications*, *12*(1), 1612. https://doi.org/10.1038/s41467-021-21857-2

Eyring, V., Bony, S., Meehl, G. A., Senior, C. A., Stevens, B., Stouffer, R. J., & Taylor, K. E. (2016). Overview of the coupled model intercomparison project phase 6 (CMIP6) experimental design and organization. *Geoscientific Model Development*, *9*(5), 1937–1958. https://doi.org/10.5194/gmd-9-1937-2016

Fang, X., & Chen, N. (2022). Quantifying the predictability of ENSO complexity using a statistically accurate multiscale stochastic model and information theory. *Journal of Climate*, 1–49.

Frauen, C., & Dommenget, D. (2012). Influences of the tropical Indian and Atlantic oceans on the predictability of ENSO. *Geophysical Research Letters*, *39*(2), L02706. https://doi.org/10.1029/2011gl050520

Ham, Y. G., Kug, J. S., & Park, J. Y. (2013a). Two distinct roles of Atlantic SSTs in ENSO variability: North tropical Atlantic SST and Atlantic Niño. *Geophysical Research Letters*, *40*(15), 4012–4017. https://doi.org/10.1002/grl.50729

Ham, Y. G., Kug, J. S., Park, J. Y., & Jin, F. F. (2013b). Sea surface temperature in the north tropical Atlantic as a trigger for El Niño/southern oscillation events. *Nature Geoscience*, *6*(2), 112–116. https://doi.org/10.1038/ngeo1686

Hasselmann, K. (1976). Stochastic climate models Part I. Theory. *Tellus*, *28*(6), 473–485. https://doi.org/10.1111/j.2153-3490.1976.tb00696.x

Hou, M., Duan, W., & Zhi, X. (2019). Season-dependent predictability barrier for two types of El Niño revealed by an approach to data analysis for predictability. *Climate Dynamics*, *53*(9), 5561–5581. https://doi.org/10.1007/s00382-019-04888-w

Jansen, M. F., Dommenget, D., & Keenlyside, N. (2009). Tropical atmosphere–Ocean interactions in a conceptual framework. *Journal of Climate*, *22*(3), 550–567. https://doi.org/10.1175/2008jcli2243.1

Jeong, H.-I., Ahn, J.-B., Lee, J.-Y., Alessandri, A., & Hendon, H. H. (2015). Interdecadal change of interannual variability and predictability of two types of ENSO. *Climate Dynamics*, *44*(3–4), 1073–1091. https://doi.org/10.1007/s00382-014-2127-3

Jeong, H.-I., Lee, D. Y., Ashok, K., Ahn, J.-B., Lee, J.-Y., Luo, J.-J., et al. (2012). Assessment of the APCC couple MME suite in predicting the distinctive climate impacts of two flavors of ENSO during boreal winter. *Climate Dynamics*, *39*(1–2), 475–493. https://doi.org/10.1007/s00382-012-1359-3

Jiang, L., & Li, T. (2021). Impacts of Tropical North Atlantic and equatorial Atlantic SST anomalies on ENSO. *Journal of Climate*, *34*(14), 5635–5655. https://doi.org/10.1175/jcli-d-20-0835.1

Jin, E. K., Kinter, J. L., Wang, B., Park, C. K., Kang, I. S., Kirtman, B. P., et al. (2008). Current status of ENSO prediction skill in coupled ocean–atmosphere models. *Climate Dynamics*, *31*(6), 647–664. https://doi.org/10.1007/s00382-008-0397-3

Jin, F. F. (1997a). An equatorial ocean recharge paradigm for ENSO. Part I: Conceptual model. *Journal of the Atmospheric Sciences*, *54*(7), 811–829. https://doi.org/10.1175/1520-0469(1997)054<0811:aeorpf>2.0.co;2

Jin, F. F. (1997b). An equatorial recharge paradigm for ENSO. Part II: A stripped-down coupled model. *Journal of the Atmospheric Sciences*, *54*(7), 830–8847. https://doi.org/10.1175/1520-0469(1997)054<0830:aeorpf>2.0.co;2

Jin, Y., & Liu, Z. (2021). A theory of the spring persistence barrier on ENSO. Part I: The role of ENSO period. *Journal of Climate*, *34*(6), 2145–2155. https://doi.org/10.1175/jcli-d-20-0540.1

Jin, Y., Liu, Z., Lu, Z., & He, C. (2019). Seasonal cycle of background in the tropical Pacific as a cause of ENSO spring persistence barrier. *Geophysical Research Letters*, *46*(22), 13371–13378. https://doi.org/10.1029/2019gl085205

Jin, Y., Lu, Z., & Liu, Z. (2020). Controls of spring persistence barrier strength in different ENSO regimes and implications for 21st century changes. *Geophysical Research Letters*, *47*(11), e2020GL088010. https://doi.org/10.1029/2020gl088010

Keenlyside, N. S., Ding, H., & Latif, M. (2013). Potential of equatorial Atlantic variability to enhance El Niño prediction. *Geophysical Research Letters*, *40*(10), 2278–2283. https://doi.org/10.1002/grl.50362

Keenlyside, N. S., & Latif, M. (2007). Understanding equatorial Atlantic interannual variability. *Journal of Climate*, *20*(1), 131–142. https://doi.org/10.1175/jcli3992.1

Kim, H. M., Webster, P. J., & Curry, J. A. (2009). Impact of shifting patterns of Pacific Ocean warming on North Atlantic tropical cyclones. *Science*, *325*(5936), 77–80. https://doi.org/10.1126/science.1174062

Kim, J. W., & Yu, J. Y. (2022). Single- and multi-year ENSO events controlled by pantropical climate interactions. *npj Climate and Atmospheric Science*, *5*(1), 88. https://doi.org/10.1038/s41612-022-00305-y

Kug, J., Jin, F., & An, S. (2009). Two types of El Niño events: Cold Tongue El Niño and warm pool El Niño. *Journal of Climate*, *22*(6), 1499–1515. https://doi.org/10.1175/2008jcli2624.1

Latif, M., Anderson, D., Barnett, T., Cane, M., Kleeman, R., Leetmaa, A., et al. (1998). A review of the predictability and prediction of ENSO. *Journal of Geophysical Research*, *103*(C7), 14375–14393. https://doi.org/10.1029/97jc03413

Liu, Z., & Di Lorenzo, E. (2018). Mechanisms and predictability of Pacific decadal variability. *Current Climate Change Reports*, *4*(2), 128–144. https://doi.org/10.1007/s40641-018-0090-5

Losada, T., Rodríguez-Fonseca, B., Janicot, S., Gervois, S., Chauvin, F., & Ruti, P. (2010). A multi-model approach to the Atlantic equatorial mode: Impact on the West African monsoon. *Climate Dynamics*, *35*(1), 29–43. https://doi.org/10.1007/s00382-009-0625-5

Martín-Rey, M., Polo, I., Rodríguez-Fonseca, B., & Kucharski, F. (2012). Changes in the interannual variability of the tropical Pacific as a response to an equatorial Atlantic forcing. *Science Marina*, *76*(S1), 105–116. https://doi.org/10.3989/scimar.03610.19a

Martín-Rey, M., Rodríguez-Fonseca, B., & Polo, I. (2015). Atlantic opportunities for ENSO prediction. *Geophysical Research Letters*, *42*(16), 6802–6810. https://doi.org/10.1002/2015gl065062

Martín-Rey, M., Rodríguez-Fonseca, B., Polo, I., & Kucharski, F. (2014). On the Atlantic–Pacific Niños connection: A multidecadal modulated mode. *Climate Dynamics*, *43*(11), 3163–3178. https://doi.org/10.1007/s00382-014-2305-3

McPhaden, M. J. (2004). Evolution of the 2002/03 El Niño. *Bulletin of the American Meteorological Society*, *85*(5), 677–696. https://doi.org/10.1175/bams-85-5-677

Meinen, C. S., & McPhaden, M. J. (2000). Observations of warm water Volume changes in the equatorial Pacific and their relationship to El Niño and La Niña. *Journal of Climate*, *13*(20), 3551–3559. https://doi.org/10.1175/1520-0442(2000)013<3551:oowwvc>2.0.co;2

Mu, M., Xu, H., & Duan, W. (2007). A kind of initial errors related to "spring predictability barrier" for El Niño events in Zebiak-Cane model. *Geophysical Research Letters*, *34*(3), L03709. https://doi.org/10.1029/2006gl027412

Newman, M., Alexander, M. A., & Scott, J. D. (2011). An empirical model of tropical ocean dynamics. *Climate Dynamics*, *37*(9), 1823–1841. https://doi.org/10.1007/s00382-011-1034-0

Newman, M., & Sardeshmukh, P. D. (2017). Are we near the predictability limit of tropical Indo-Pacific sea surface temperatures? *Geophysical Research Letters*, *44*(16), 8520–8529. https://doi.org/10.1002/2017gl074088

Penland, C., & Matrosova, L. (1994). A balance condition for stochastic numerical models with application to the El Nino-Southern Oscillation. *Journal of Climate*, *7*(9), 1352–1372. https://doi.org/10.1175/1520-0442(1994)007<1352:abcfsn>2.0.co;2

Penland, C., & Sardeshmukh, P. D. (1995). The optimal-growth of tropical sea-surface temperature anomalies. *Journal of Climate*, *8*(8), 1999–2024. https://doi.org/10.1175/1520-0442(1995)008<1999:togots>2.0.co;2

Polo, I., Martin-Rey, M., Rodriguez-Fonseca, B., Kucharski, F., & Mechoso, C. R. (2015). Processes in the Pacific La Niña onset triggered by the Atlantic Niño. *Climate Dynamics*, *44*(1–2), 115–131. https://doi.org/10.1007/s00382-014-2354-7

Polo, I., Rodríguez-Fonseca, B., Losada, T., & García-Serrano, J. (2008). Tropical Atlantic variability modes (1979–2002). Part I: Time-evolving SST modes related to West African rainfall. *Journal of Climate*, *21*(24), 6457–6475. https://doi.org/10.1175/2008jcli2607.1

Ren, H. L., & Jin, F. F. (2011). Niño indices for two types of ENSO. *Geophysical Research Letters*, *38*(4). https://doi.org/10.1029/2010gl046031

Ren, H.-L., Jin, F.-F., Song, L., Lu, B., Tian, B., Zuo, J., et al. (2017). Prediction of primary climate variability modes in Beijing Climate Center. *Journal of Meteorological Research*, *31*(1), 204–223. https://doi.org/10.1007/s13351-017-6097-3

Ren, H. L., Jin, F.-F., Tian, B., & Scaife, A. A. (2016). Distinct persistence barriers in two types of ENSO. *Geophysical Research Letters*, *43*(20), 10973–10979. https://doi.org/10.1002/2016gl071015

Ren, H. L., Zuo, J., & Deng, Y. (2019). Statistical predictability of Niño indices for two types of ENSO. *Climate Dynamics*, *52*(9–10), 5361–5382. https://doi.org/10.1007/s00382-018-4453-3

Rodríguez-Fonseca, B., Polo, I., García-Serrano, J., Losada, T., Mohino, E., Mechoso, C., & Kucharski, F. (2009). Are Atlantic Ni?os enhancing Pacific ENSO events in recent decades. *Geophysical Research Letters*, *36*(20), L20705. https://doi.org/10.1029/2009GL040048

Smith, T. M., & Reynolds, R. W. (2004). Improved extended reconstruction of SST (1854–1997). *Journal of Climate*, *17*(12), 2466–2477. https://doi.org/10.1175/1520-0442(2004)017<2466:ieros>2.0.co;2

Steiger, J. H. (1980). Test for comparing elements of correlations matrix. *Psychological Bulletin*, *87*, 45–281.

Tang, Y., Zhang, R. H., Liu, T., Duan, W., Yang, D., Zheng, F., et al. (2018). Progress in ENSO prediction and predictability study. *National Science Review*, *5*(6), 826–839. https://doi.org/10.1093/nsr/nwy105

Tao, L. J., Gao, C., & Zhang, R. H. (2019). Model parameter-related optimal perturbations and their contributions to El Niño prediction errors. *Climate Dynamics*, *52*(3–4), 1425–1441. https://doi.org/10.1007/s00382-018-4202-7

Tseng, Y.-H., Huang, J.-H., & Chen, H.-C. (2022). Improving the predictability of two types of ENSO by the characteristics of extratropical precursors. *Geophysical Research Letters*, *49*(3), e2021GL097190. https://doi.org/10.1029/2021gl097190

Vecchi, G. A., & Harrison, D. E. (2000). Tropical Pacific sea surface temperature anomalies, El Niño, and equatorial westerly wind events. *Journal of Climate*, *13*(11), 1814–1830. https://doi.org/10.1175/1520-0442(2000)013<1814:tpssta>2.0.co;2

Wang, L., Yu, J.-Y., & Paek, H. (2017). Enhanced biennial variability in the Pacific due to Atlantic capacitor effect. *Nature Communications*, *8*(1), 14887. https://doi.org/10.1038/ncomms14887

Webster, P. J., & Yang, S. (1992). Monsoon and ENSO: Selectively interactive systems. *Quarterly Journal of the Royal Meteorological Society*, *118*(507), 877–926. https://doi.org/10.1002/qj.49711850705

Wu, R., Kirtman, B. P., & van den Dool, H. (2009). An analysis of ENSO prediction skill in the CFS retrospective forecasts. *Journal of Climate*, *22*(7), 1801–1818. https://doi.org/10.1175/2008jcli2565.1

Xie, S. P., & Carton, J. A. (2013). Tropical Atlantic variability: Patterns, mechanisms, and impacts. In *Earth's climate: The ocean–atmosphere interaction*. In *Geophysical monograph series* (Vol. 147, pp. 121–142). Amer. Geophys. Union.

Xue, Y., Cane, M., Zebiak, S., & Blumenthal, M. (1994). On the prediction of ENSO: A study with a low-order markov model. *Tellus*, *46*(4), 512–528. https://doi.org/10.3402/tellusa.v46i4.15641

Zebiak, S. E. (1993). Air–sea interaction in the equatorial Atlantic region. *Journal of Climate*, *6*(8), 1567–1586. https://doi.org/10.1175/1520-0442(1993)006<1567:aiitea>2.0.co;2

Zhao, Y., Jin, Y., Li, J., & Capotondi, A. (2022). The role of extratropical Pacific in crossing ENSO spring predictability barrier. *Geophysical Research Letters*, *49*(15), e2022GL099488. https://doi.org/10.1029/2022gl099488

Zheng, F., & Yu, J. Y. (2017). Contrasting the skills and biases of deterministic predictions for the two types of El Niño. *Advances in Atmospheric Sciences*, *34*(12), 1395–1403. https://doi.org/10.1007/s00376-017-6324-y